A distribution network planning model considering neighborhood energy trading

(Article begins on next page)

17 April 2024

A Distribution Network Planning Model Considering Neighborhood Energy Trading

Javid Maleki Delarestaghi, Ali Arefi, Gerard Ledwich, Alberto Borghetti

Abstract— **The widespread adoption of small-scale distributed energy resources (DERs) amongst energy users has drastically changed the operation of distribution networks. To date, there has not been a consolidated model to incorporate the investment decisions of the end-users in the distribution network planning. The contribution of this paper is a distribution network planning model for the utility which considers the neighborhood energy trading (NET) as a platform for end-users to directly exchange energy between them. The proposed mixed-integer second-order cone programming (MISOCP) problem provides the optimal decisions for line and transformer upgrades, as well as for photovoltaic (PV) and battery in users' premises. Moreover, it indicates a fair allocation of network charges among the participants to NET schemes. The simulation results on the IEEE-33 bus test system confirm the effectiveness of the proposed model in lowering the total cost of the planning and the operation. This platform can be used by government-owned utilities as a guide to avoid sunk investments while motivating the increased installation of renewable distributed generation and storage units by end-users.**

Index Terms— **distribution network planning, electricity market, local energy community, prosumers' engagement, renewables, storage.**

I. NOMENCLATURE

Indices

t	index for time intervals
s	index for cluster
i or j	indices for end-users, buses, or branches
π	index of candidate choices for replacing a line
ξ	index of candidate choices of transformers to be installed
w	index of candidate choices of PV units to be installed
k	index of candidate choices of battery units to be installed
h	index of auxiliary variables for linearization

Sets

T	set of time intervals
S	set of clusters
N	set of end-users, buses, or branches
Π	set of candidate choices for replacing lines
Ξ	set of candidate choices for transformers to be installed
W	set of candidate choices of PV units to be installed
K	set of candidate choices of battery units to be installed
$\overline{x_u}/\overline{x_c}$	set of investment decision variables for utility/end-users
$\overline{y_u}/\overline{y_c}$	set of operational variables for utility/end-users
$\overline{y_s}$	set of power flow calculation variables

Parameters

$CL_{i\pi}$	investment cost of candidate replacing line π in branch i
CT_ξ	investment cost of candidate transformer ξ
n	number of end-users/buses/branches
CPV_w	investment cost of candidate PV unit w
CB_k	investment cost of candidate battery unit k
ρ_s	probability of cluster s in planning
ω_{ts}	wholesale price in time interval t and cluster s ($/MWh)
R_{ts}	retail price in time interval t and cluster s ($/MWh)
L_{ts}	energy price for NET in cluster s and time interval t ($/MWh)
DF_i	disutility factor for user i ($/MWh)
CC_{i0}	cost to end-user i without NET
CC_{u0}	minimum cost to utility without NET
A_{ij}	ij-th element of bus injection to branch current (BIBC) matrix
RM_{ij}	ij-th element of matrix RM whose value is equal to product of A_{ij} and the resistance of j-th branch
XM_{ij}	ij-th element of matrix XM whose value is equal to product of A_{ij} and the reactance of j-th branch
V_0	substation voltage (in p.u.)
MR_{ij}	ij-th element of matrix MR whose value is equal to product of A_{ji} and the resistance of j-th branch
MX_{ij}	ij-th element of matrix MX whose value is equal to product of A_{ji} and the reactance of j-th branch
MZ_{ij}	ij-th element of matrix MZ whose value is equal to product of A_{ji} and the square impedance magnitude of j-th branch
q_{its}	reactive power drawn by end-user i in time interval t and cluster s (MVAr)
$\overline{V}/\underline{V}$	maximum/minimum allowed voltage
$I_{max}^{\pi/\overline{i0}}$	maximum allowed current of (candidate line π)/(branch i)
$I_{max}^{\xi/00}$	maximum allowed current of (candidate transformer ξ)/(substation transfomer)
η_c/η_d	charging/discharging efficiency of battery units
SoC_k^{max}	maximum state of charge of candidate battery k
SoC_k^{min}	minimum state of charge of candidate battery k
M	large enough positive value to relax constraints (big-M method)
pc_k^{max}	maximum charging power of candidate battery k
pd_k^{max}	maximum discharging power of candidate battery k
G_{iwts}	output of candidate PV unit w at bus i in time interval t and cluster s (MWh)
BD_i	degradation unit cost of battery at bus i ($/cycle)
D_{its}	demand at bus i in time interval t and cluster s (MWh)
d_{its}^{max}	maximum allowable demand to be shifted by end-user i from time interval t in cluster s (MWh)
t_{max}	number of time intervals
n_h	number of digits for nc

Variables

$x_l^{i\pi}$	binary variable which shows whether branch i is replaced by a line of type π
x_{TR}^ξ	binary variable which shows whether the substation transformer is upgraded by a new transformer of type ξ
x_{PV}^{iw}	binary variable which shows whether a PV of type j is installed by end-user i
x_B^{ik}	binary variable which shows whether a battery of type k is installed by end-user i
P_{1ts}	active power at the sending end of the first branch in time interval t and cluster s (MW)
pr_{its}	purchased energy from utility by end-user i in time interval t and cluster s (MWh)
pl_{its}^+/pl_{its}^-	purchased/sold energy in NET mechanism by end-user i in time interval t and cluster s (MWh)
nc_{ts}	network charge in time interval t and cluster s ($/MWh)

BDC_i	degradation cost of the battery at bus i ($/MWh)
d_{its}	shiftable load of end-user i from time interval t in cluster s (MWh)
p_{its}^c	nodal injection of battery charging energy by end-user i in time interval t and cluster s (MWh)
p_{its}^d	nodal injection of battery discharging energy by end-user i in time interval t and cluster s (MWh)
P_{its}/Q_{its}	active/reactive power at the sending end of branch i in time interval t and cluster s (MW)
u_{its}	square current magnitude in line i, time interval t and cluster s
v_{its}	square voltage magnitude at bus i in time interval t and cluster s
$v_{\underline{i}ts}$	square voltage magnitude at sending end of branch i in time interval t and cluster s ((kV)^2)
SoC_{its}	battery state of charge of at bus i in time interval t and cluster s (MWh)
$SoC_{i,max}$	maximum state of charge of battery at bus i
$SoC_{i,min}$	minimum state of charge of battery at bus i
α_{its}	binary variable which determines the charging state of the battery at bus i, in time interval t and cluster s ($\alpha_{its}=1$ means the battery is in charging state)
β_{its}	auxiliary variable which shows a change in charging state of the battery at bus i, in time interval t and cluster s
$p_{i,max}^c$	maximum charging power of the battery at bus i
$p_{i,max}^d$	maximum discharging power of the battery at bus i
BNC_i^B	number of charging-discharging cycles of the battery at bus i
z_{its}	binary variable which shows whether end-user i consumes (0) or produces (1) energy in time interval t
nc_{tsh}	auxiliary binary variable corresponding to network charge level in time interval t and cluster s ($/MWh)
$e_{itsh}^{\pm}$	auxiliary variable of network charge for end-user i in time interval t and cluster s ($)

Functions

f	objective function
INV/OPR	total investment/operating cost
INV_u/INV_c	total investment cost incurred to the utility/end-users
INV_c^i/OPR_c^i	i-th end-user's investment/operating cost
OPR_u	total operating cost incurred to the utility
OPR_c	total operating cost incurred to end-users
$\Psi/\widehat{\Psi}$	power flow and network operational constraints
$\Upsilon/\widehat{\Upsilon}$	end-users' operational constraints

II. Introduction

The distribution network (DN) planning investigates the investment decisions that the grid owner needs to make in order to retain the technical criteria of the network at the minimum cost. The transition of end-users from passive energy consumers towards small-scale active prosumers with distributed energy resources (DERs), i.e. end-users that both consume and produce energy, provides new challenges for DN planners. End-users with DERs can form a local energy community (LEC) which could help in the operation of the DN. In an LEC, there are various ways for end-users to supply their demand, i.e. buying from the utility, using the DERs in their own premises, or buying the energy from other end-users in a neighborhood energy trading (NET) scheme.

The NET offers exceptional opportunities for end-users to make value from underutilized assets in the grid and to exploit opportunities to install new renewable generation and storage units. For example, it may be more convenient for some NET participants not to invest in DERs because they can use the excess PV generation or storage facilities of their neighbors. However, there might be cases

in which more investment in DERs is profitable because of the significant demand level in the LEC. Besides, the utility may adopt congestion management schemes that include the utilization of DERs in end-users' premises. However, it would not be efficient if the utility does not consider the investment decisions of end-users in their own energy-related decisions. This may lead to over/under-investment and, consequently, higher network costs, as already been experienced in, e.g., Australia [1] and European Union [2]. This paper presents a planning model for the utility that incorporates the prosumers' engagement in NET schemes in order to acquire the optimal investment plan.

A. Literature review

The application of modern optimization procedures to power system planning is well documented in the literature. The application of mixed-integer nonlinear programming (MINLP) to the DN planning with the alternatives of investment in feeder upgrade, distributed generation (DG), and wind turbines is studied in [3], using a robust algorithm to address the uncertainties and convexification to guarantee the global optimality of the solution. Reference [4] proposes a co-optimization model by incorporating the investment decisions on DGs besides the conventional alternatives and operational costs in active DNs (ADNs). A multi-year ADN planning model including both traditional and smart grid technologies is presented in [5]. The authors in [6] propose a model for coordinated planning of MV and LV DNs considering DG penetration at the MV level. In [7], a risk-managed planning model is developed using both network and non-network solutions to find the least cost investment plan for utilities. A two-stage planning method for ADNs is investigated in [8] that optimizes several planning alternatives as well as the active management of DGs.

The concept of joint investment planning for DNs is also an explored topic in the literature. The joint planning of network infrastructure and private-owned DG installation has been analyzed in [9-12] to find a suitable investment plan for the utility and other self-interested entities or individuals. A similar approach has been adopted in [13] to model a cooperative investment planning of multi-microgrids and then to propose a cost-sharing scheme for a fair allocation of the capital costs among the microgrids. The planning problem of the DN and the investments in the microgrid development are addressed in [14] by a coordinated approach to allow the further adoption of PV units while maintaining the operational limits of the network. The influence of electricity prices on the investment decisions is discussed in, e.g., [15-17] for the planning of transmission networks under the market environment.

To the best of our knowledge, the impact of energy trading among end-users on the investment planning of DNs has not yet been dealt with in the literature. This is the original contribution of the present paper.

B. Contribution

Building upon the analysis presented in [18], this paper is based on the consideration that NET schemes, if allowed, should be taken into account in utility's decisions since the impact is expected to be significant.

In this framework, the contributions of this paper are:
1) presentation of a model for the optimal planning of utility's investments that incorporates the expected end-users' investments in DERs;
2) inclusion of the NET scheme in the DN planning;
3) optimum design of the network charge (NC);

4) demonstration of the computational features of the developed mixed-integer second-order cone programming (MISOCP) model by using the IEEE 33-bus system as a test case

This study outlines the optimal DN planning pathway considering the expected investment decisions of end-users. With this in mind, any deviation in end-users' investment decisions can be treated as a source of uncertainty in the problem. This model is a useful tool for government-owned utilities that are seeking the benefit of their societies (minimizing the total cost of electrification). The expected outcome of end-users' investment decisions can be negotiated with them either directly or via agreements through an aggregator.

III. PROBLEM DESCRIPTION AND FORMULATION

The investment of NET participants in DERs is driven mainly by the specific NET rules and opportunities, while the utility mainly considers the grid investment plan to tackle peak loads. These different aims are aligned in the framework proposed in this paper by considering both the utility and end-users' costs and benefits. Although the model is represented by a centralized decision-making unit for the utility, the results can be a useful guide also to facilitate the implementation of NET schemes, since the proposed model guarantees that all NET participants will benefit by cooperating with other parties in the NET.

Due to the integrality characteristic of investment decisions and the nonconvexity of power flow equations, we need to deal with a mixed-integer nonlinear programming (MINLP) model. It has been reported in several studies, e.g., [19], that relaxing some nonconvex constraints greatly facilitates finding global optima. To this end, a mixed-integer second-order cone programming (MISOCP) model is proposed, which can be efficiently handled by available optimizers.

The following subsections A, B, and C discuss the considerations regarding the NC, the objective function, and the constraints of the proposed MISOCP model respectively, whilst subsection D is devoted to the adopted solution approach. The results of the numerical tests are presented in Section IV.

A. Network charge

The NC for the end-users that do not participate in the NET is normally regulated by, e.g., the national regulator who sets the tariff. However, the NET participants use the network for selling or buying energy, and hence should be charged accordingly. The NC in this study is what the NET participants will pay to the utility. The utility sets the NC only to rationalize the appropriate use of network infrastructure, not to maximize its profit. Since the utility is not treated as a profit-making entity here, the minimum NC is obtained along with other investments with the objective to minimize the total cost of electrification. The utility may reward some of the NET participants if they contribute to the reduction of network stress.

The simple and conventional NC is a constant fee during the day regardless of the actual requirements for maintaining the network operational condition. This type of NC is not expected to efficiently influence the electricity market and reflect the grid demand. This design is named static NC (SNC). The utility can better avert the risk of congestion or avoid network upgrades by introducing a more elaborate NC design, called dynamic NC (DNC). The DNC better reflects the costs borne by the utility. The proposed framework in this study also includes the optimization of a DNC scheme.

B. Objective function

For simplicity, we consider that the utility acts both as the DN operator and the energy provider to the end-users. The local gener-

ation is provided only by PV units. Since we consider only one radial feeder connected to the main substation, the total power request is the power at the sending end of the first line, i.e. P_{1ts}. The duration of each time interval is 1 hour.

To model the uncertainties in the optimization horizon T, the profiles of loads, PV generation and electricity prices over the planning period are categorized into several representative day scenarios, denoted as cluster s, each with probability ρ_s, by employing the k-means method presented in [20], as illustrated in Section IV.

The objective function described in (1) is the total investment (INV) and operating costs (OPR), as described in the two sets of equations (2)-(5) and (6)-(9), respectively.

$$\min f(\overline{x_u}, \overline{x_c}, \overline{y_u}, \overline{y_c}, \overline{y_s}) = INV(\overline{x_u}, \overline{x_c}) + OPR(\overline{y_u}, \overline{y_c}, \overline{y_s}) \quad (1)$$

where

$$INV(\overline{x_u}, \overline{x_c}) = INV_u + INV_c \quad (2)$$

$$INV_u = \sum_{\pi \in \Pi} \sum_{i \in N} CL_{i\pi} x_l^{i\pi} + \sum_{\xi \in \Xi} CT_\xi x_{TR}^\xi \quad (3)$$

$$INV_c = \sum_{i=1}^n INV_c^i \quad (4)$$

$$INV_c^i = \sum_{w \in W} CPV_w x_{PV}^{iw} + \sum_{k \in K} CB_k x_B^{ik} \quad (5)$$

$$OPR(\overline{y_u}, \overline{y_c}, \overline{y_s}) = OPR_u + OPR_c \quad (6)$$

$$OPR_u = \sum_{s \in S} \rho_s \left[\sum_{t \in T} \omega_{ts} P_{1ts} - \sum_{t \in T} \sum_{i=1}^n R_{ts} pr_{its} \right. \quad (7)$$
$$\left. - \sum_{t \in T} \sum_{i \in N} (pl_{its}^+ + pl_{its}^-) nc_{ts} \right]$$

$$OPR_c = \sum_{i \in N} OPR_c^i \quad (8)$$

$$OPR_c^i = \sum_{s \in S} \rho_s \left[\sum_{t \in T} R_{ts} pr_{its} + \sum_{t \in T} (nc_{ts} + L_{ts}) pl_{its}^+ \right. \quad (9)$$
$$+ \sum_{t \in T} (nc_{ts} - L_{ts}) pl_{its}^- + BDC_i$$
$$\left. + DF_i \sum_{t \in T} d_{its} \right]$$

As shown in (3) and (6), line and transformer reinforcement for the utility as well as the PV and battery installation for prosumers are considered as investment alternatives and are denoted by $x_l^{i\pi}$, x_{TR}^ξ, x_{PV}^{iw}, and x_B^{ik}, respectively. The utility's operating cost includes the cost of energy purchases from the wholesale market, revenue (negative cost) of selling energy to consumers, and the revenue of network charge, as detailed in (7).

The prosumers' operating cost in (9) includes, for each time interval t and cluster s, the cost of energy purchases from the utility ($R_{ts} pr_{its}$), the cost of energy purchases from NETs ($L_{ts} pl_{its}^+$), the revenue of energy sold in NETs ($-L_{ts} pl_{its}^-$), the cost of battery depreciation (BDC_i), and the disutility cost of prosumers due to the application of DR that requires changes in their scheduled demand ($DF_i d_{its}$). The price in NET schemes depends on quantities available and therefore is a function of circumstances, but, for the sake of simplicity, it is considered static here, equal to the average values forecasted by the utility for the different time periods.

The network charge during time interval t is modeled as nc,

which can be SNC or DNC: The SNC corresponds to a constant value of nc_{ts} during the optimization horizon, while the DNC corresponds to a scheme in which the value of nc_{ts} may vary in different time intervals.

The variables are divided into 5 groups based on their type (investment, operational, or power flow variables) and side (utility or prosumers):

$$\bar{x}_c = \{x_{PV}^{iw}, x_B^{ik} | \forall i \in N, \forall w \in W, \forall k \in K\} \qquad (10)$$

$$\overline{x_u} = \{x_l^{i\pi}, x_{TR}^{\xi} | \forall \pi \in \Pi, \forall \xi \in \Xi, \forall i \in N\} \qquad (11)$$

$$\bar{y}_c = \{pr_{its}, pl_{its}^{\pm}, d_{its}, p_{its}^c, p_{its}^d | \forall i \in N, \forall t \in T, \forall s \in S\} \qquad (12)$$

$$\overline{y_u} = \{nc_{ts}, P_{1ts} | \forall t \in T, \forall s \in S\} \qquad (13)$$

$$\bar{y}_s = \{P_{its}, Q_{its}, u_{its}, v_{its} | \forall i \in N, \forall t \in T, \forall s \in S\} \qquad (14)$$

The sets of decision variables of end-users ($\bar{x}_c$) and the utility ($\overline{x_u}$) contain the investment in PV (x_{PV}^{iw}), battery (x_B^{ik}), new line ($x_l^{i\pi}$) and new transformer (x_{TR}^{ξ}). The sets of operational variables of end-users ($\bar{y}_c$), of the utility ($\overline{y_u}$), and of those of the power flow equations ($\bar{y}_s$) include the amount of energy purchased from the utility by each end-user (pr_{its}), the amount of energy sold or purchased in NET ($pl_{its}^{\pm}$), the amount of battery charging and discharging (p_{its}^c, p_{its}^d), DR decisions (d_{its}), the network charge level for the participants in NET schemes (nc_{ts}), the amount of energy purchased from the wholesale market (P_{1ts}), the power flows in lines (P_{its}, Q_{its}), the square magnitude of line currents (u_{its}) and the square magnitude of bus voltages (v_{its}).

C. Constraints

The model includes the following sets of equality and inequality constraints.

$$\Psi(\overline{x_u}, \bar{y}_c, \bar{y}_s) \geq 0, \quad \widehat{\Psi}(\overline{x_u}, \bar{y}_c, \bar{y}_s) = 0 \qquad (15)$$

$$\Upsilon(\bar{x}_c, \overline{y_u}, \bar{y}_c) \geq 0, \quad \widehat{\Upsilon}(\bar{x}_c, \overline{y_u}, \bar{y}_c) = 0 \qquad (16)$$

$$INV_c^i + OPR_c^i \leq CC_{i0} \quad \forall i \in N, \qquad (17)$$
$$INV_u + OPR_u \leq CC_{u0}$$

The constraints associated with the power flow equations and network operational constraints are included in (15). The users' operational constraints are represented in (16). The constraints in (17) ensure that the utility and the end-users will participate in the NET market only if it is beneficial to them, with CC_{i0} and CC_{u0} calculated by the optimization model forbidding NETs.

The detailed description of each set of constraints is provided below by omitting, for the sake of brevity, their validity for $\forall i \in N, \forall t \in T$, and $\forall s \in S$.

The power flow and network operational constraints in (15) are detailed in (18)-(23), based on the convex model presented in [21] for networks with radial configuration. Without considering the bus at the substation, the number of buses is equal to the number of branches (i.e., n). Each bus at the receiving end of a branch and the branch itself are indicated with the same label.

$$P_{its} = \sum_{j=1}^{n} \left(A_{ij}\left(pr_{jts} + pl_{jts}^+ - pl_{jts}^-\right) + RM_{ij}u_{jts} \right) \qquad (18)$$

$$Q_{its} = \sum_{j=1}^{n} \left(A_{ij}q_{jts} + XM_{ij}u_{jts} \right) \qquad (19)$$

$$v_{its} = V_0^2 - 2\sum_{j=1}^{n} \left(MR_{ij} P_{jts} + MX_{ij} Q_{jts} \right. \qquad (20)$$
$$\left. - 0.5MZ_{ij} u_{jts} \right)$$

$$(P_{its})^2 + (Q_{its})^2 - u_{its}v_{\underline{i}ts} \leq 0 \qquad (21)$$

$$\left(\underline{V}\right)^2 \leq v_{its} \leq \left(\overline{V}\right)^2 \qquad (22)$$

$$\begin{cases} u_{its} \leq x_l^{i\pi}((I_{max}^{\pi})^2 - (I_{max}^{i0})^2) + (I_{max}^{i0})^2 \\ u_{0ts} \leq x_{TR}^{\xi}\left(\left(I_{max}^{\xi}\right)^2 - (I_{max}^{00})^2\right) + (I_{max}^{00})^2 \end{cases} \qquad (23)$$

where P_{its}, Q_{its}, and u_{its} are the active and reactive powers at the sending end, and the current square magnitude of branch i, respectively; v_{its} is the squared of voltage magnitude at sending end of branch i, all in time interval t in cluster s; A_{ij}, RM_{ij}, XM_{ij}, MR_{ij}, MX_{ij}, and MZ_{ij} are the ij-th elements of their corresponding square matrices and they are equal to ij-th element of the BIBC matrix of the network, the product of A_{ij} and the resistance r_j of the branch j, the product of A_{ij} and the reactance x_j of the branch j, the product of A_{ji} and the resistance of the branch j, the product of A_{ji} and the reactance of the branch j, and finally, the product of A_{ij} and the square impedance magnitude of the branch j, i.e. $r_j^2 + x_j^2$, respectively.

Constraint (18) states that the active power at the sending end of branch i is equal to the sum of the loads supplied by branch i plus the sum of the losses in all downward branches connected to branch i. Analogously, (19) is written for reactive power. Constraint (21) is the relaxed version of the link between the square of the apparent power and the square of the product of voltage and current. Constraint (22) enforces the voltage bounds. Constraint (23) applies the current limits. Constraint (20) is the matrix form of the DistFlow equation [22] of the following constraint,

$$v_{up(i)ts} - v_{its} = -2(r_iP_{its} + x_iQ_{its}) + (r_i^2 + x_i^2)u_{its} \qquad (24)$$

where $up(i)$ and i are the labels of the sending and receiving ends of branch i.

The set of constraints in (16) comprises the model of the battery operation (25)-(43), the model of the state of each prosumer (44)-(48) that avoids a prosumer from acting as a consumer and producer in the same time interval, the energy balance in NET (49), the energy balance for each end-user (50), and the limit on DR (51).

$$SoC_{its} = SoC_{i(t-1)s} + \eta_c p_{its}^c - \frac{p_{its}^d}{\eta_d} \qquad (25)$$

$$SoC_{i,max} = \sum_{k \in K} SoC_k^{max} x_B^{ik} \qquad (26)$$

$$SoC_{i,min} = \sum_{k \in K} SoC_k^{min} x_B^{ik} \qquad (27)$$

$$SoC_{its} \leq SoC_{i,max} \qquad (28)$$

$$SoC_{its} \geq SoC_{i,min} \qquad (29)$$

$$p_{its}^c \leq \alpha_{its}M \qquad (30)$$

$$p_{its}^d \leq (1 - \alpha_{its})M \qquad (31)$$

$$\beta_{its} \geq \alpha_{i(t+1)s} - \alpha_{its} \quad \forall t \in T - \{t_{max}\} \qquad (32)$$

$$\beta_{it_{max}s} \geq \alpha_{i1s} - \alpha_{it_{max}s} \tag{33}$$

$$\beta_{its} \geq \alpha_{i(t+1)s} - \alpha_{its} \qquad \forall t \in T - \{t_{max}\} \tag{34}$$

$$\beta_{it_{max}s} \geq \alpha_{i1s} - \alpha_{it_{max}s} \tag{35}$$

$$p_{i,max}^c = \sum_{k \in K} pc_k^{max} x_B^{ik} \tag{36}$$

$$p_{i,max}^d = \sum_{k \in K} pd_k^{max} x_B^{ik} \tag{37}$$

$$p_{its}^c \leq p_{i,max}^c \tag{38}$$

$$p_{its}^d \leq p_{i,max}^d \tag{39}$$

$$\eta_c \eta_d \sum_{t \in T} p_{its}^c = \sum_{t \in T} p_{its}^d \tag{40}$$

$$p_{its}^c \leq G_{iwts} x_{PV}^{iw} \tag{41}$$

$$BNC_i = 0.5 \sum_{t \in T} \beta_{its} \tag{42}$$

$$BDC_i = BD_i \, BNC_i \tag{43}$$

$$pl_{its}^- \leq M \, z_{its} \tag{44}$$

$$pl_{its}^+ \leq M \, (1 - z_{its}) \tag{45}$$

$$pr_{its} \leq M \, (1 - z_{its}) \tag{46}$$

$$D_{its} + p_{its}^c - p_{its}^d + d_{its} - \sum_{w \in W} G_{iwts} x_{PV}^{iw} \leq M(1 - z_{its}) \tag{47}$$

$$D_{its} + p_{its}^c - p_{its}^d + d_{its} - \sum_{w \in W} G_{iwts} x_{PV}^{iw} \geq -M z_{its} \tag{48}$$

$$\sum_{i \in N} (pl_{its}^+ - pl_{its}^-) = 0 \tag{49}$$

$$p_{its} + pl_{its}^+ - pl_{its}^- = D_{its} + p_{its}^c - p_{its}^d + d_{its} \\ - \sum_{w \in W} G_{iwts} x_{PV}^{iw} \tag{50}$$

$$d_{its} \leq d_{its}^{max} \tag{51}$$

The state of charge (SoC) of the battery in each time interval is calculated in (25). The maximum and minimum limits for battery SoC are calculated in (26) and (27), respectively. Equations (28) and (29) apply the limits on the SoC of the battery. The state of battery operation, i.e. charging or discharging, is found in (30) and (31). The transition from one operating state to another one is detected in (32)-(35). The charging and discharging powers are limited in (36)-(39). Constraint (40) ensures that the net energy stored in the battery in a day is zero. As the retail price is considered to be flat-rate, constraint (41) is added to ensure that the prosumers only store the excess generation of their PVs, not the energy purchases from the utility, which would clearly deteriorate their own benefits. The number of cycles of the battery is represented in (42). In (43), the depreciation cost of the battery is calculated.

Constraint (49) imposes the equality of energy purchases and sales through the NET. The constraint (50) states the balance of energy for prosumers. Finally, the amount of shifted power to/from a time interval is limited by (51).

The quadratic term $(pl_{its}^+ + pl_{its}^-) nc_{ts}$ in (9) would make the constraint matrix of the model a non-positive semi-definite matrix which is not accepted by off-the-shelf optimizers, e.g., Gurobi [23]. In order to overcome this issue, we assume that nc_{ts} is an integer number, so its equivalent binary expression is $\sum_{h=1}^{n_h} 2^{h-1} nc_{tsh} - \sum_{h=1}^{n_h} 2^{h-2}$ where $nc_{tsh} \in \{0,1\}$. Following [24], a new variable, $e_{itsh}^{\pm}$, is defined and (9) is replaced by (52)-(56), as follows

$$OPR_c^i = \sum_{s \in S} \Big[BDC_i + \sum_{t \in T} \Big(R_{its} pr_{its} + DF_i d_{its} + \\ \sum_{h=1}^{n_h} 2^{h-1} (e_{itsh}^+ + e_{itsh}^-) \Big) \Big] \tag{52}$$

and the following linear constraints are added:

$$e_{itsh}^{\pm} \leq pl_{its}^{\pm} \tag{53}$$

$$e_{itsh}^{\pm} \leq M nc_{tsh} \tag{54}$$

$$e_{itsh}^{\pm} \geq pl_{its}^{\pm} - M(1 - nc_{tsh}) \tag{55}$$

$$e_{itsh}^{\pm} \geq 0 \tag{56}$$

D. Solution approach

The algorithm to solve the proposed planning model is illuminated in Fig. 1. At first, the data of the network under study, i.e. the topology and specification of the existing and candidate replacing equipment, the load demand and PV generation data, wholesale price, retail price, the maximum available demand response of each prosumer and the interest rate are collected. Then multiple scenarios for load demand, PV generation profile, and wholesale price are generated by clustering the collected data. Finally, the input matrices of the proposed model are built to be provided to the optimization solver.

Collect the data of demands, PV profile, wholesale price

↓

Run k-means clustering to find representative day scenarios

↓

Input the parameters: network configuration, specification of equipment, retail price, network charge, feed-in tariff, candidate PV and battery specifications, available demand response

↓

Form the distribution network planning model in (1)-(8) and (10)-(56)

| Utility's investment in poles and wires | ↔ | Neighborhood energy trading scheme | ↔ | Investment in DERs at end-users' premises |

↓

Initiate solving the planning model in Gurobi using the branch and bound and barrier techniques

↓

Set S=original planning problem with relaxed integrality constraints, $B = \emptyset$, $LB = -\infty$, $UB = +\infty$, $OS = \emptyset$

↓

1- for s in S
  2- perform the optimization of s
    3- if feasible then
      4- denote the optimal solution as α^* and best objective as s^*
      5- update $LB = \min\{LB, s^*\}$
      6- if α^* satisfies all integrality constraints then
        7- if $UB \geq s^*$ then
          8- update $UB = s^*$ and $OS = \alpha^*$
      9- else then
        10- update $B = B \cup \{s\}$
    11- else then $s = S$. Next and return to 1
12- set $S = \emptyset$
13- branch on branching variables for $\forall b \in B$ and add the produced subproblems to S
14- if ($S \neq \emptyset$ and $|UB - LB| \geq \varepsilon$) then return to 1, else then print OS as the optimal solution and UB as the best objective
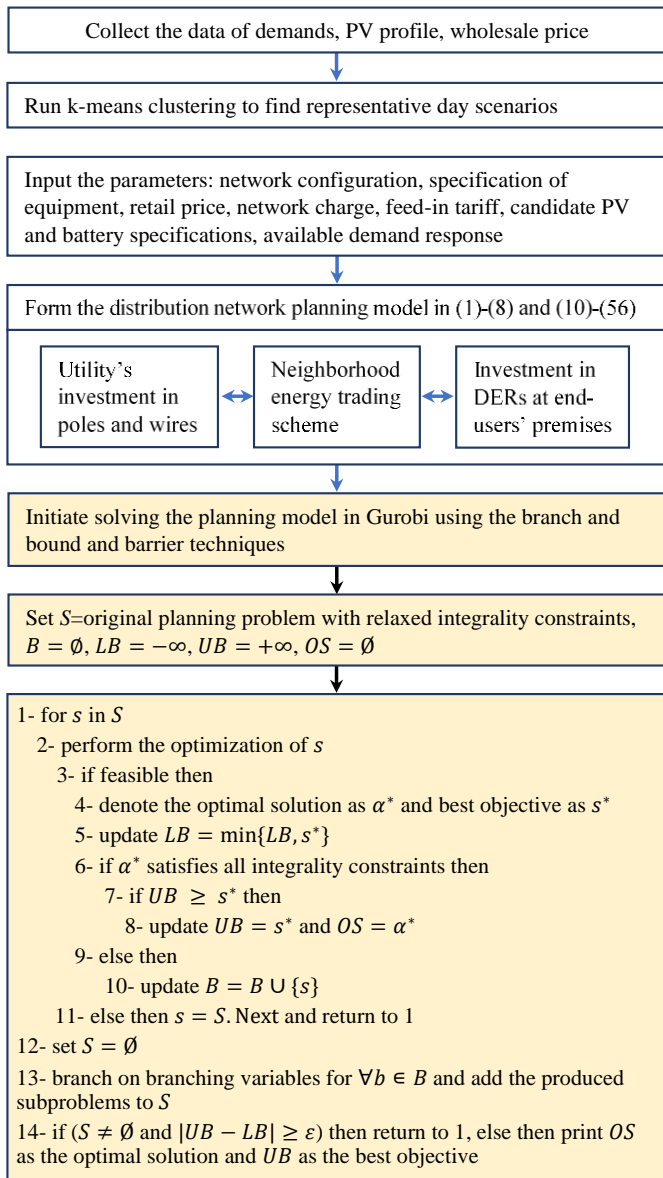
Fig. 1. Flowchart of the proposed method

To obtain the results of Section IV, the procedure has been implemented in Matlab and the Gurobi 8.0.0 solver has been adopted. The calculations have been carried out by using an Intel CORE i5-2500 PC with the clock speed 3.30 GHz and 8GB RAM.

As mentioned in [19], the Gurobi solver implements a combination of two methods, branch-and-bound (BB) and barrier, to address the integrality and solving the relaxed SOCP model, respectively. In this regard, the MISOCP model is relaxed to an SOCP model by assuming the integer variables to be continuous. The SOCP is solved by the barrier method and the optimal solution is checked to see if the integrality constraints are maintained. The solution of the relaxed model is a lower bound (LB) for the original problem. The BB continues the solution by branching on the integer variables that do not satisfy the integrality constraints. Any optimal solution of the generated sub-problems that satisfies the optimality constraints is an upper bound (UB) of the original MISOCP problem. The algorithm stops branching if the gap between UB and LB falls below the threshold or the maximum allowed iteration number is reached.

IV. CASE STUDIES AND ANALYSIS OF THE RESULTS

The considered case studies are based on the IEEE 33-bus radial test system with data provided in Table 1 of [25]. In Fig. 2, the candidate locations for PV and battery installations are represented by the PV and battery icon. The input parameters are listed in TABLE I, where the rates and costs are obtained from [26, 27]. The electricity price in NET is assumed to be constant at 15 cents per kWh, a value between the retail price and the feed-in tariff offered by the utility. Due to the constant retail price, end-users are not interested to store the energy purchased from the utility and use it later. Thus, the battery is only used to store the excess energy generated by PV. For the sake of simplicity, the efficiency of battery charging/discharging is assumed 100%.
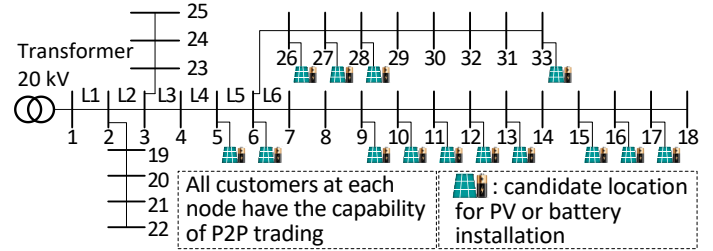

Fig. 2. IEEE 33-bus test network

parameter	value
retail price ($/MWh)	240
feed-in-tariff ($/MWh)	60
local price ($/MWh)	150
static network charge ($/MWh)	50
7kW PV unit investment cost ($)	8500
7kWh-3kW battery unit investment cost ($)	4000
new line fixed investment cost (k$)	75
new line per km investment cost (k$/km)	75
New 5 MVA transformer investment cost (k$)	350
operating voltage (kV)	20
expected lifetime of PV and battery (year)	10
expected lifetime of new lines (year)	40
O&M cost of battery ($/MWh)	20
disutility factor for consumers' DR ($/MWh)	40
interest rate (%)	4

Two schemes of NC are examined, namely, SNC and DNC, represented as described in section III.

Due to the intrinsic incentive of the NET (cheaper energy compared to the retail market), the prosumers are expected to shift their load demand to the time intervals when the NET market is more active, i.e., to the hours of significant PV generation. Therefore, we consider the end-users can shift their load from peak hours in the evening to daytime, namely the load shift is allowed from (18:00 – 03:00) to (08:00 – 17:00), but the reverse is not allowed.

A. Clustering output

By applying the k-means data clustering over one year, 3 representative days (denoted as clusters) are determined for the load demand, PV generation, and the wholesale electricity price. The data of load demand and wholesale price are collected from [28], and the PV generation profiles are obtained based on weather forecast data [29], for one year starting from 1 Dec 2017. Each cluster represents the daily per unit profiles of load demand, PV generation, and the wholesale market price, as seen in Fig. 3. The probability of each cluster is shown in TABLE II, in which cluster 3 would represent 52% of a year.
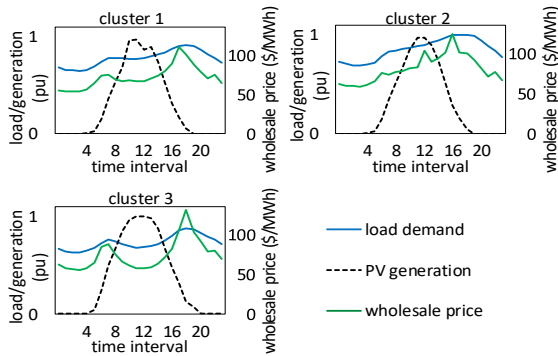
Fig. 3. Three clusters representing one year

TABLE II
PROBABILITY OF CLUSTERS

	cluster 1	cluster 2	cluster 3
probability (%)	31	17	52

The wholesale price reasonably tracks the load demand in all clusters. The electricity price drops in the middle of the day with high PV generation in clusters 1 and 3. The peak of the wholesale electricity price occurs at 17:00, 16:00, and 18:00 in clusters 1, 2, and 3, respectively.

Considering the terms in (1)-(9), the objective function can be classified into 4 groups. These cost terms and the parameters that affect them are listed in TABLE III. The critical decisions, which are centrally optimized, and the corresponding effective parameters are also shown in TABLE III. The obtained clusters effectively represent the parameters mentioned in TABLE III. For example, cluster 3 contains the peak price, the peak PV generation, and the maximum PV generation duration, whilst cluster 2 exhibits the peak load. Therefore, these clusters can be considered proper for planning optimization.

TABLE III
IMPORTANT PARAMETERS IN CLUSTERING

Cost terms		Effective parameters
utility investment		peak load
prosumer investment		PV generation, electricity price, load level
utility operations	wholesale purchase	electricity price
	network power loss	load level
prosumer operations		electricity price, load level, PV generation
max power traded in NET		peak PV generation
max daily energy traded in NET		duration of PV generation
max DR		peak load
max battery usage		peak load and peak price

B. Cases

The planning procedure is applied to 7 different cases, as shown in TABLE IV. The effect of the presence of NET with both the SNC and DNC designs, as well as the impact of considering the cost for only either utility or end-users to the planning results is analyzed.

TABLE IV
DESCRIPTION OF SIMULATION CASES (✓ FUNCTION PRESENT, ✗ NOT PRESENT)

	P2P trading	Dynamic network charge (DNC)	Objective function	
			utility cost: (3)+(6)	customers cost: (4)+(8)
case 1	✗	✗	✓	✓
case 2	✓	✓	✓	✗
case 3	✓	✓	✗	✓
case 4	✓	✓	✓	✓
case 5	✓	✗	✓	✗
case 6	✓	✗	✗	✓
case 7	✓	✗	✓	✓

Optimization results for the total installed capacity of PV and

battery and the total number of upgraded line sections are listed in TABLE V. The utility's cost, total end-users' cost, and total cost of electrification are illustrated in Fig. 4. The results are discussed in the following sub-sections.

TABLE V
RESULTS OF INVESTMENT DECISIONS

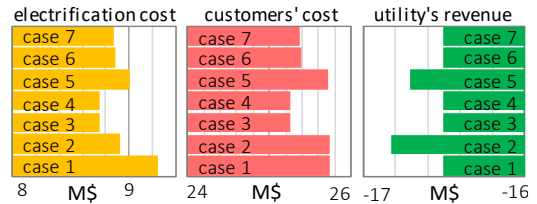| Case #	1	2	3	4	5	6	7
Total PV (kW)	952	1029	3108	3108	826	1099	1113
Total battery (kWh)	0	70	434	434	266	35	0
New line sections	2	1	0	0	1	1	1

Fig. 4. Optimization results

C. The impact of NET

We compare case 1 in which NET is not allowed, with the corresponding cases that enable NET: case 4 (with DNC) and case 7 (with SNC). As shown in Fig. 4, the total cost of electrification decreases by enabling the NET. End-users' cost in case 4 and 7 is lower than case 1 because they can buy or sell in NETs at a more convenient price. The utility's revenue is not reduced by NETs, since two-line sections must be upgraded in case 1, while there is no line upgrade in case 4, and only one line section is replaced in case 7.

The end-users' investments in batteries are triggered in all cases with NET, while in case 1 no battery is installed. Moreover, the end-users are more willing to invest in PV units in case 4 and case 7 when compared to case 1. Particularly in case 4, a considerable capacity of PV (3.26 times more than in case 1) is installed by end-users. It shows that the NET is a proper incentive for the end-users to increase the use of renewables.

D. The impact of including the end-users' costs

The total cost in case 4 is lower than in case 2, which considers only the utility's costs in the objective function, and is equal to that of case 3, which minimizes only the end-users' costs. Also, the size of PV and battery units calculated by the optimization procedure in case 4 matches that of case 3. While the total installed capacity of PV and battery units in case 4 is 3 times higher than case 2, the end-users' cost in case 4 is lower than case 2. With SNC, analogous considerations are obtained by comparing the results of case 7 with those of case 5 and case 6. The total electrification cost and the total end-users' cost in case 7 are lower than in case 5, while the total installed capacity of PV systems in case 7 is 35% higher than in case 5.
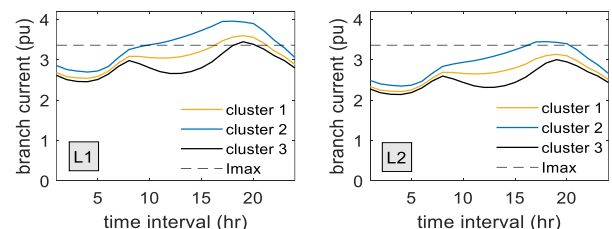

Fig. 5. Daily current flows through L1 and L2 in all clusters in case 1.

Fig. 5 shows the current magnitude in branches L1 and L2 in case 1. The currents exceed the maximum limit from 9:00 to 22:00 and 17:00 to 20:00, in L1 and L2, respectively. To find out how it

is avoided in case 4, a detailed illustration of the energy consumption and production is presented in Fig. 6 in all clusters.
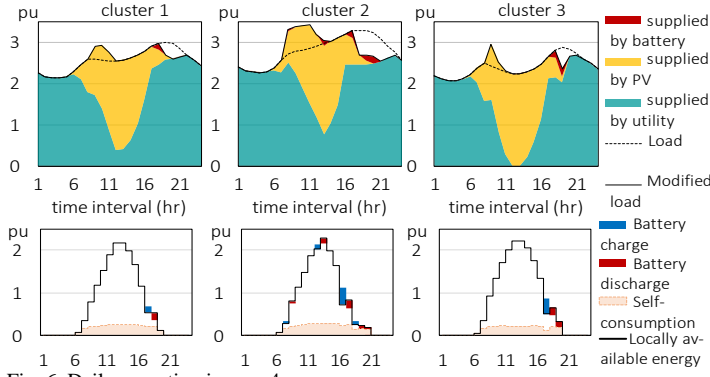

Fig. 6. Daily operation in case 4

The mitigation of congestion in lines is addressed in two ways: increase in production by prosumers and the activation of DR. The former one happens over the day and has a peak during the midday when 99% of load demand is supplied locally at 12:00 and 13:00 in cluster 3. The latter one has a significant impact on investment deferral, as the peak load which determines the need for poles and wires upgrade occurs in time intervals when the PV generation is zero. As shown in Fig. 6, NET motivates the end-users to shift their load demand in all clusters so to alleviate the congestion in L1 and L2. The difference between the load and the modified load in Fig. 6 shows the amount of load shifted by end-users. End-users shift their load from 19:00-21:00 to 9:00-11:00 in clusters 1 and 3 and from 18:00-23:00 to 8:00-13:00 in cluster 2 (i.e., from when the sun goes down and the production of PV is around zero to the morning and early in the afternoon where cheap energy is available in the NET). The active cooperation of end-users and the utility in case 4 benefits both prosumers and utility to handle the grid congestions and avoid any grid upgrade.
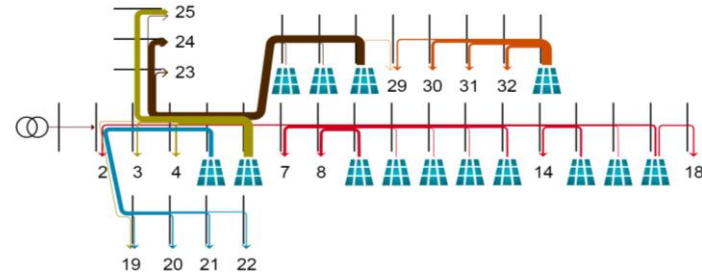

Fig. 7. Energy flows at 12 PM in cluster 3 and case 4

The energy flow at 12:00 in cluster 3 and case 4 is illustrated in Fig. 7. In this case, the load demand balances the local production to a great extent (99%). The small amount of power imported by the utility is mostly due to the grid losses.

E. The impact of DNC

Comparing case 2 with case 5, case 3 with case 6, and case 4 with case 7, the total electrification cost decreases by employing DNC, as shown in Fig. 5. This improvement is expected as the search space (the feasible region) of the optimization problem is expanded in cases with DNC compared with those that adopt SNC.

The resulted DNC level for case 4 is shown in Fig. 8 for all clusters. The level of NC is at its highest value, $75 per MWh, and on some occasions, it drops to lower values. For example, the load and wholesale price are at their peak during 18:00-19:00 in clusters 1 and 3, thus the utility offers a negative NC that is an incentive to

the end-users to participate in the NET in order to avoid line upgrades and to avoid importing power from the upstream grid at high wholesale prices. Moreover, the utility offers a negative NC at 17:00-20:00 in cluster 2 mainly to avoid L1 and L2 upgrade due to peak load.
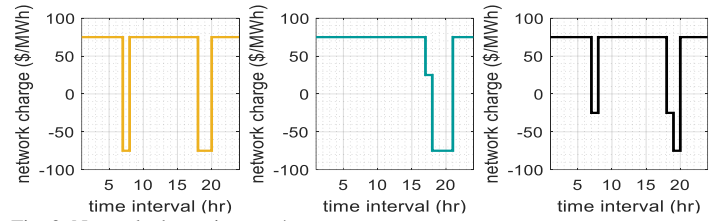

Fig. 8. Network charge in case 4

For case 4, the impact of DNC on battery installation and battery operation is shown in Fig. 6: batteries are discharged at 18:00 in cluster 1, at 17:00 and 19:00 in cluster 2, and at 18:00 and 19:00 in cluster 3, when all have negative NC rate. In other words, the utility encourages the prosumers to discharge the energy stored in their batteries by placing a negative NC tariff. Normally, the utility prefers the batteries to discharge during the peak demand and charge during off-peak periods [30], which is satisfied with DNC.

F. Details of end-users' investment

The total end-users' cost is listed in TABLE VI. Also, the size and location of investments in PV and battery units by end-users are shown in Table VII. There is a strong relationship between the capacity of installed PV/battery units by an end-user and the load level around its location. In case 4, the capacity of installed PV/battery units is significantly higher at buses 5, 6, 28, and 33 which are close to buses with a high level of load demand, compared to other candidate locations.

The cost incurred to the end-user at bus 6 drops by 35% in case 4 as compared to case 1 due to the 389% increase in PV installation and participating in the NET. When comparing case 4 to case 1 for the end-user located at bus 27, the overall prosumers' cost decreases by 2% while the installed PV capacity drops by 56%. This highlights the function of NET in preventing the end-users from both under and overinvestments.

TABLE VI
DETAILED CUSTOMERS COST IN CASE 1 AND CASE 4

bus #	2	3	4	5	6	7	8	9	10	11	12
case 1	829	746	995	118	118	1658	1658	118	118	29	118
case 4	821	723	973	98	76	1636	1640	100	116	29	116
bus #	13	14	15	16	17	18	19	20	21	22	23
case 1	118	995	118	118	118	746	746	746	746	746	746
case 4	116	970	118	117	118	739	740	732	742	729	733
bus #	24	25	26	27	28	29	30	31	32	33	
case 1	3481	3481	118	118	118	995	1658	1243	1741	353	
case 4	3425	3432	116	115	90	981	1633	1212	1709	353	

TABLE VII
INVESTMENT DECISIONS

Case #	End-users' investment		Utility's investment
	PV: busbar#(kW)	Battery: busbar#(kWh)	
1	5(63), 6(63), 9(63), 10(63), 11(14), 12(63), 13(63), 15(63), 16(63), 17(63), 26(63), 27(63), 28(63), 33(182)	none	L1, L2
2	5(35), 6(35), 9(35), 10(28), 11(7), 12(35), 13(42), 15(56), 16(35), 17(483), 26(35), 27(42), 28(35), 33(126)	17(70)	L1
3	5(294), 6(553), 9(238), 10(28), 11(7), 12(28), 13(175), 15(133), 16(35), 17(189), 26(28), 27(28), 28(672), 33(700)	6(49), 10(14), 12(7), 13(49), 15(35), 16(14), 17(35), 33(231)	none
4	5(308), 6(630), 9(210), 10(28), 11(21), 12(28), 13(133), 15(154), 16(28), 17(231), 26(28), 27(28), 28(581), 33(700)	5(7), 11(7), 13(35), 15(49), 16(7), 17(70), 28(42), 33(217)	none
5	5(35), 6(35), 9(42), 10(42), 11(189), 12(42), 13(49), 15(49), 16(35), 17(56), 26(35), 27(42), 28(35), 33(140)	9(7), 10(14), 11(98), 12(7), 13(14), 15(28), 16(7), 17(21), 27(7), 28(7), 33(56)	L1
6	5(35), 6(35), 9(35), 10(35), 11(14), 12(35), 13(35), 15(56), 16(49), 17(105), 26(35), 27(35), 28(56), 33(539)	15(7), 17(28)	L1
7	5(35), 6(35), 9(35), 10(35), 11(455), 12(35), 13(35), 15(35), 16(35), 17(35), 26(35), 27(35), 28(35), 33(238)	none	L1

G. Probabilistic analysis of voltage and loss

Probabilistic voltage profile and power losses are shown in Fig. 9 for case 4. As seen, the 95% confidence interval for voltage magnitudes lies within the ±5% of the nominal voltage. As expected, the buses far from the substation experience more variation and deviation from the nominal voltage. The jump in voltage profile from bus 18 to 19 is due to the network configuration shown in Fig. 2.
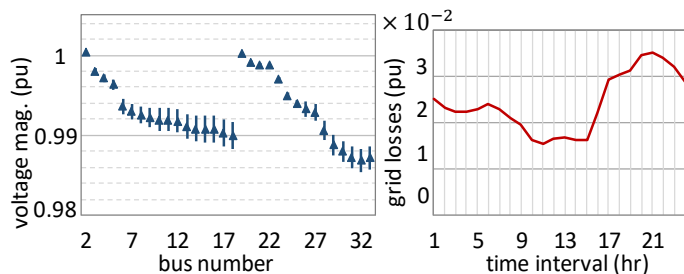

Fig. 9. Voltage magnitude with 95% confidence interval for one year and the grid loss during a typical day in case 4

The profile of the average grid losses reminds the so-called "duck-curve" demand profile which highlights the strong correlation between the level of loading and the grid losses. The average grid losses are always lower than 0.035 per unit with a base value of 100MVA.

H. Computational performance

As expected, the required time for convergence of this programming problem depends on the size of the problem (number of variables and number of constraints) and the value of the input parameters. For the network considered in this paper with 31,344 variables for case 4, the computation time is 51 min with the maximum gap threshold between LB and UB equal to 0.05%. The computation time is 12 min and 14 seconds for case 7 with 21,984 variables and for case 1 with 19,680 variables, respectively. These computation time values are considered reasonable for planning studies.

I. Extension to multi-year planning

As mentioned, the results shown in this paper refers to a one-year planning horizon, represented by 3 clusters. The planning framework can be extended to a multi-year period using the forward-backward method presented in [7]. This method finds an optimal solution for the multi-year planning problem by efficiently decomposing it into a sequence of one-year planning problems in a combined form of forward and backward planning.

V. CONCLUSION

An investment plan for the utility that considers the decisions of energy users in the distribution network, specifically regarding neighborhood energy trades (NET), is presented in this paper. Other than the investment of the utility in grid reinforcement, the proposed model also incorporates the calculation of the optimal investment in PV and battery units in order to provide a guide for the utility to motivate the increased installation of these units by end-users. The model also considers a dynamic network charge (DNC) mechanism, considering the uncertainties associated with load demand, wholesale price, and PV generation.

The model is adapted in a convex MISOCP problem that can be efficiently handled by the available optimization solvers. The results obtained for different case studies based on the IEEE 33-bus test system verifies the efficiency and applicability of the proposed approach. The results show that NET prevents the prosumers and the utility from over/underinvestment by offering a platform that provides energy at more convenient prices for both the buyers and the sellers. Moreover, the utility can defer the upgrade of poles and wires by guiding the NET via designing proper DNC. Further work needs to focus on the inclusion of reliability of the system [31], the risk of present uncertainties , and the application of the proposed model in establishment of virtual power plants [32].

REFERENCES

[1]　Australian Competition & Consumer Commission, "Restoring electricity affordability & Australia's competitive advantage," 2018. [Online]. Available: https://www.accc.gov.au/publications/restoring-electricity-affordability-australias-competitive-advantage

[2]　S. Pront-van Bommel, "A reasonable price for electricity," *Journal of Consumer Policy,* vol. 39, no. 2, pp. 141-158, 2016.

[3]　N. Amjady, A. Attarha, S. Dehghan, and A. J. Conejo, "Adaptive Robust Expansion Planning for a Distribution Network With DERs," *IEEE Transactions on Power Systems,* vol. 33, no. 2, pp. 1698-1715, 2018, doi: 10.1109/tpwrs.2017.2741443.

[4]　X. Shen, M. Shahidehpour, S. Zhu, Y. Han, and J. Zheng, "Multi-Stage Planning of Active Distribution Networks Considering the Co-Optimization of Operation Strategies," *IEEE Transactions on Smart Grid,* vol. 9, no. 2, pp. 1425-1433, 2018, doi: 10.1109/tsg.2016.2591586.

[5]　S. Mohtashami, D. Pudjianto, and G. Strbac, "Strategic Distribution Network Planning with Smart Grid Technologies," *IEEE Transactions on Smart Grid,* vol. 8, no. 6, pp. 2656-2664, 2017, doi: 10.1109/tsg.2016.2533421.

[6]　R. Gholizadeh-Roshanagh, S. Najafi-Ravadanegh, and S. H. Hosseinian, "A Framework for Optimal Coordinated Primary-Secondary Planning of Distribution Systems Considering MV Distributed Generation," *IEEE Transactions on Smart Grid,* vol. 9, no. 2, pp. 1408-1415, 2018, doi: 10.1109/tsg.2016.2590425.

[7]　A. Arefi, A. Abeygunawardana, and G. Ledwich, "A New Risk-Managed Planning of Electric Distribution Network

Incorporating Customer Engagement and Temporary Solutions," *IEEE Transactions on Sustainable Energy,* vol. 7, no. 4, pp. 1646-1661, 2016, doi: 10.1109/tste.2016.2573290.

[8] N. C. Koutsoukis, P. S. Georgilakis, and N. D. Hatziargyriou, "Multistage Coordinated Planning of Active Distribution Networks," *IEEE Transactions on Power Systems,* vol. 33, no. 1, pp. 32-44, 2018, doi: 10.1109/tpwrs.2017.2699696.

[9] G. Munoz-Delgado, J. Contreras, and J. M. Arroyo, "Joint Expansion Planning of Distributed Generation and Distribution Networks," *IEEE Transactions on Power Systems,* vol. 30, no. 5, pp. 2579-2590, 2015, doi: 10.1109/tpwrs.2014.2364960.

[10] M. Asensio, P. M. de Quevedo, G. Muñoz-Delgado, and J. Contreras, "Joint distribution network and renewable energy expansion planning considering demand response and energy storage—Part I: Stochastic programming model," *IEEE Transactions on Smart Grid,* vol. 9, no. 2, pp. 655-666, 2016.

[11] M. Asensio, P. M. de Quevedo, G. Muñoz-Delgado, and J. Contreras, "Joint distribution network and renewable energy expansion planning considering demand response and energy storage—Part II: Numerical results," *IEEE Transactions on Smart Grid,* vol. 9, no. 2, pp. 667-675, 2016.

[12] J. Contreras, M. Asensio, P. M. de Quevedo, G. Muñoz-Delgado, and S. Montoya-Bueno, *Joint RES and Distribution Network Expansion Planning under a Demand Response Framework.* Academic Press, 2016.

[13] H. Wang and J. Huang, "Cooperative Planning of Renewable Generations for Interconnected Microgrids," *IEEE Transactions on Smart Grid,* vol. 7, no. 5, pp. 2486-2496, 2016, doi: 10.1109/tsg.2016.2552642.

[14] M. Armendáriz, M. Heleno, G. Cardoso, S. Mashayekh, M. Stadler, and L. Nordström, "Coordinated microgrid investment and planning process considering the system operator," *Applied Energy,* vol. 200, pp. 132-140, 2017, doi: 10.1016/j.apenergy.2017.05.076.

[15] Y. Gu and J. McCalley, "Market-based transmission expansion planning," presented at the 2011 IEEE/PES Power Systems Conference and Exposition, Phoenix, AZ, USA, 20-23 March 2011, 2011.

[16] F. D. Munoz, B. F. Hobbs, J. L. Ho, and S. Kasina, "An Engineering-Economic Approach to Transmission Planning Under Market and Regulatory Uncertainties: WECC Case Study," *IEEE Transactions on Power Systems,* vol. 29, no. 1, pp. 307-317, 2014, doi: 10.1109/tpwrs.2013.2279654.

[17] J. H. Zhao, J. Foster, Z. Y. Dong, and K. P. Wong, "Flexible Transmission Network Planning Considering Distributed Generation Impacts," *IEEE Transactions on Power Systems,* vol. 26, no. 3, pp. 1434-1443, 2011, doi: 10.1109/tpwrs.2010.2089994.

[18] J. M. Delarestaghi, A. Arefi, and G. Ledwich, "The impact of peer to peer market on energy costs of consumers with pv and battery," presented at the 2018 IEEE PES Innovative Smart Grid Technologies Conference Europe (ISGT-Europe), Sarajevo, Bosnia and Herzegovina, Bosnia and Herzegovina, 21-25 Oct. 2018, 2018.

[19] S. Burer and A. N. Letchford, "Non-convex mixed-integer nonlinear programming: A survey," *Surveys in Operations Research and Management Science,* vol. 17, no. 2, pp. 97-106, 2012, doi: 10.1016/j.sorms.2012.08.001.

[20] S. Lloyd, "Least squares quantization in PCM," *IEEE transactions on information theory,* vol. 28, no. 2, pp. 129-137, 1982.

[21] M. Farivar and S. H. Low, "Branch flow model: Relaxations and convexification—Part I," *IEEE Transactions on Power Systems,* vol. 28, no. 3, pp. 2554-2564, 2013.

[22] M. Baran and F. F. Wu, "Optimal sizing of capacitors placed on a radial distribution system," *IEEE Transactions on power Delivery,* vol. 4, no. 1, pp. 735-743, 1989.

[23] *Gurobi Optimizer Reference Manual*. (2018). [Online]. Available: http://www.gurobi.com

[24] A. Billionnet, S. Elloumi, and A. Lambert, "Exact quadratic convex reformulations of mixed-integer quadratically constrained problems," *Mathematical Programming,* vol. 158, no. 1-2, pp. 235-266, 2015, doi: 10.1007/s10107-015-0921-2.

[25] M. E. Baran and F. F. Wu, "Network reconfiguration in distribution systems for loss reduction and load balancing," *IEEE Transactions on Power delivery,* vol. 4, no. 2, pp. 1401-1407, 1989.

[26] AEMC, "2018 Residential Electricity Price Trends, Final report, 21 December 2018," 2018.

[27] S. C. P. Ltd. "Residential Solar PV Price Index – February 2019." https://www.solar-choice.net.au/blog/51210/blog/residential-solar-pv-price-index-february-2019/ (accessed.

[28] A. E. M. Operator. *Data Dashboard*.

[29] M. Bureau Meteorol., VIC, Australia, online. *Climate information for solar energy*.

[30] A. Azizivahed *et al.*, "Risk-Oriented Multi-Area Economic Dispatch Solution with High Penetration of Wind Power Generation and Compressed Air Energy Storage System," *IEEE Transactions on Sustainable Energy,* 2019.

[31] A. Arefi, G. Ledwich, G. Nourbakhsh, and B. Behi, "A Fast Adequacy Analysis for Radial Distribution Networks Considering Reconfiguration and DGs," *IEEE Transactions on Smart Grid,* 2020.

[32] B. Behi, A. Baniasadi, A. Arefi, A. Gorjy, P. Jennings, and A. Pivrikas, "Cost–benefit analysis of a virtual power plant including solar PV, flow battery, heat pump, and demand management: A Western Australian case study," *Energies,* vol. 13, no. 10, p. 2614, 2020.